Nuclear magnetic resonance imaging: a review[1]

Richard G Henderson BSC MRCP
NMR Unit, Department of Diagnostic Radiology
Royal Postgraduate Medical School, Hammersmith Hospital, London W12 0HS

X-ray computed tomography (CT) has now been available for ten years, but the last three years have seen the emergence of a new and quite different imaging technique – nuclear magnetic resonance or NMR. At present, there are no known hazards associated with NMR, although certain precautions recommended by the National Radiological Protection Board (1981) are observed. The images produced are most appropriately compared with X-ray CT (Steiner 1982) and in certain cases with two-dimensional ultrasound. After the initial studies, it is clear that NMR is a significant new imaging modality, the importance of which is only beginning to be realized.

Historical outline

Although NMR had been used for spectroscopy for many years, following its discovery over thirty years ago (Bloch 1946, Purcell *et al.* 1946), its possible medical value was not realized until Damadian (1971) found that rat tumours *in vitro* had different NMR characteristics compared with normal tissue. This was later confirmed *in vivo* (Weisman *et al.* 1972).

The formation of images by NMR was first suggested by Damadian (1971), but the technique now used stems from work by Lauterbur (1973) who coined the term 'zeugmatography'. Subsequently, images were produced by Mansfield and his colleagues (1974) at Nottingham University. Three years later a good quality image of the human wrist was produced by Hinshaw *et al.* (1977), also working at Nottingham. This was soon followed by further images, and Damadian produced a whole-body scan using his focused NMR (FONAR) technique (Damadian *et al.* 1977). In 1978 a whole-body scan using zeugmatography was published (Mansfield *et al.* 1978) and in the same year EMI produced their first head scan (Hounsfield 1980). The groups active in the UK at present are at Nottingham (Holland *et al.* 1980 *a,b,* Hawkes *et al.* 1981 *a,b*), Aberdeen (Edelstein *et al.* 1980, Smith *et al.* 1981 *a,b,c,* 1982) and at Hammersmith (Doyle *et al.* 1981 *a,b,* Young *et al.* 1981 *a,b,* 1982). Several groups in the USA have also contributed to clinical studies (Alfidi *et al.* 1982, Buonanno *et al.* 1982, Crooks *et al.* 1982, Ross *et al.* 1982).

Physical basis and instrumentation

An NMR imaging system requires a large-bore magnet capable of accepting the human body. The body is surrounded by a radiofrequency transmitter coil which may also act as a receiver (Figure 1) in order to detect the NMR signal.

The patient must lie relatively still within the magnet for an hour or so, although each individual slice is scanned in three to eight minutes. These long scanning times may be reduced in future, especially by the technique of multiple slicing whereby several adjacent slices are scanned simultaneously.

NMR images depend on the behaviour of hydrogen nuclei (protons) – mostly from water – in a magnetic field. Protons have magnetization associated with them and so may be compared with a bar magnet. If a body is placed in a static magnetic field, the magnetization associated with the protons is preferentially aligned in the direction of the field. Should the magnetization be perturbed from this position, it precesses around the axis of the field in a manner analogous to a spinning top precessing around the vertical axis (Figure 2). This

[1]Accepted 26 July 1982

0141–0768/83/030206–07/$01.00/0

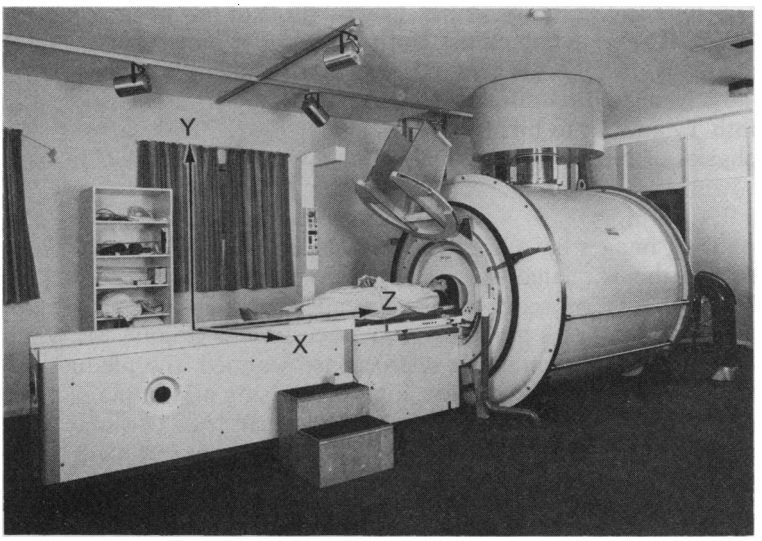

Figure 1. A cryogenic magnet NMR scanner. The patient is about to be placed within the cryogenic magnet. The radiofrequency transmitter and receiver coils surround the patient's head. The patient is lying in the longitudinal or Z axis; the X and Y axes are also marked

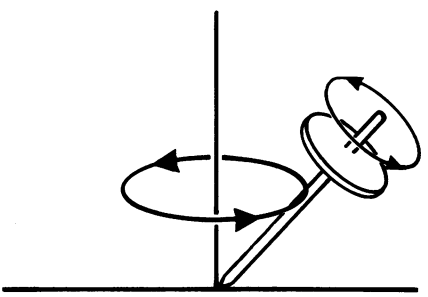

Figure 2. Precession of a spinning top. As a top spins on its axis it also rotates or precesses around the vertical axis. This may be compared with the precession of the magnetization associated with protons, which occurs at a radiofrequency around the Z axis

precession occurs at a radiofrequency (RF) known as the Larmor frequency, which varies proportionately with the magnetic field strength. When a magnetic field alternating at the Larmor frequency is applied orthogonal to the static field, the angle of rotation of the precessing magnetization can be changed. By adjusting the duration or the intensity of this RF pulse, rotation to any desired angle can be obtained.

After the application of the RF pulse, the magnetization returns exponentially or 'relaxes' to its original alignment. As it does so it continues to precess and this motion can be detected as an induced current in a receiver coil arranged around the body. The relaxation is defined by two time constants, T_1 and T_2, which describe relaxation in the longitudinal or Z axis and transverse or X-Y plane respectively (Figure 1). T_1, or spin-lattice relaxation time, is related to loss of energy from the protons to their environment; whereas T_2, or spin-spin relaxation time, is related to energy exchange between the protons.

As the Larmor frequency is proportional to the magnetic field strength, it can be seen that if a body is placed in a gradient magnetic field, a certain frequency will define a particular distance along the body. Using three orthogonal gradients, spatial labelling or encoding can be obtained.

Using a variety of sequences involving RF pulses, images can be obtained which depend on proton density, T_1 or T_2. The values of T_1 and T_2 are approximately equal (a few seconds) in

liquids, whereas in solids T_1 is long (a few minutes) and T_2 very short (a few microseconds). T_2 is always less than or equal to T_1, and in human tissues the values of T_1 are between about 150 and 1000 milliseconds. This is an absolute limiting factor in reducing scanning times. Contrast in the images is largely related to differences in T_1 and T_2 between tissues, and pathology usually causes both T_1 and T_2 to be prolonged.

A fuller account of the physics of NMR is given in a recent review (Pykett *et al.* 1982).

Brain and spinal cord

The most dramatic and promising images have been those of the brain. White matter has a shorter T_1 than grey matter, and this is related to the presence of protons in phospholipids such as myelin (Doyle *et al.* 1981*a*). As a consequence, T_1-dependent images show grey-white matter contrast which enables detailed brain anatomy to be seen *in vivo* (Figure 3). When patients with demyelinating disease such as multiple sclerosis are scanned, the plaques are visible as areas of prolonged T_1 within the white matter (Figure 4). Using NMR, many more plaques are visible than on comparable CT scans (Young *et al.* 1981*b*). The ability to distinguish myelinated from unmyelinated nerve tissue also allows the progress of maturation in the child's brain to be followed. Delayed neurological development may thus be correlated with delayed myelination. This may prove to be a very useful clinical application.

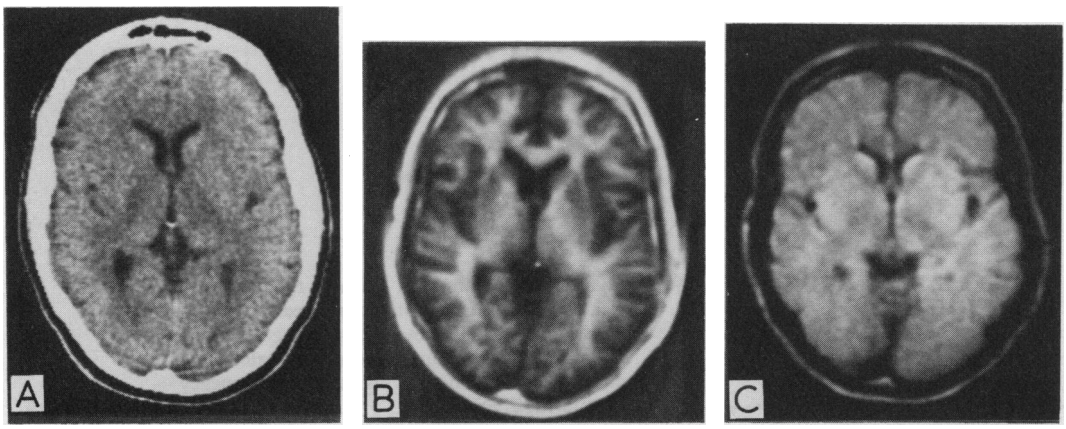

Figure 3. Comparable CT (A), T_1 (B) and T_2 (C) scans of the normal brain at low ventricular level. The T_1 image shows clear grey-white matter differentiation. The inner and outer tables of the skull give a low signal and appear dark, but subcutaneous fat and bone marrow appear light. The T_2 image shows less anatomical detail

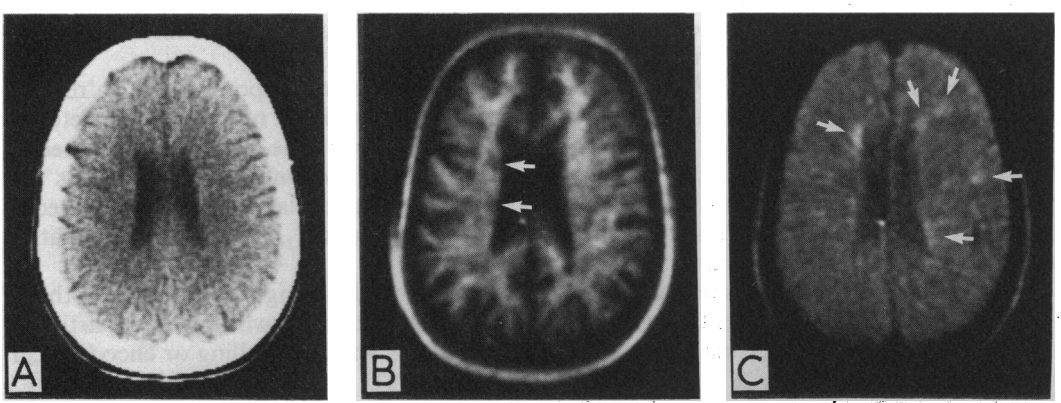

Figure 4. Comparable CT (A), T_1 (B) and T_2 (C) scans of a patient with multiple sclerosis. No lesions are visible on the CT scan, but several are seen on the T_1 scan, two of which are arrowed. The T_2 scan shows further lesions

T_2 is approximately equal in grey and white matter. Thus T_2-dependent images give much less anatomical detail than T_1 (Figure 3). However, T_2 is a sensitive indicator of pathological change (Bailes *et al.* 1982). Pathology visualized by NMR in the brain includes infarction, tumour, aneurysm and haematoma (Doyle *et al.* 1981*a*, Bailes *et al.* 1982, Bydder & Steiner 1982).

Bone contains few hydrogen nuclei, so giving a low NMR signal, and appears dark in the images (Young *et al.* 1981*a*). This means that the posterior fossa can be visualized without streak artefacts due to the thick surrounding bone, which can make CT scans difficult to interpret (Figure 5). Moreover, the proton-rich marrow does give a strong signal, and so the diploë can be seen (see especially Figure 3B), which may be of value in future studies of bone pathology.

By adjusting the gradient fields, coronal and sagittal NMR scans may be obtained directly without the need for reconstruction from multiple transverse slices (Holland *et al.* 1980*a*). Brain images obtained in this way (Figure 6) show great detail, and sagittal sections of the spine (Figure 7) allow the vertebrae and discs to be visualized. More detailed scans showing the spinal cord and nerve roots will soon be available.

Figure 5. T_1 scan of a normal subject at the level of the pons. Anteriorly the lens of each eye is seen. The slice includes the anterior part of the temporal lobes, the pons, fourth ventricle (arrowed), cerebellar peduncles and cerebellar hemispheres

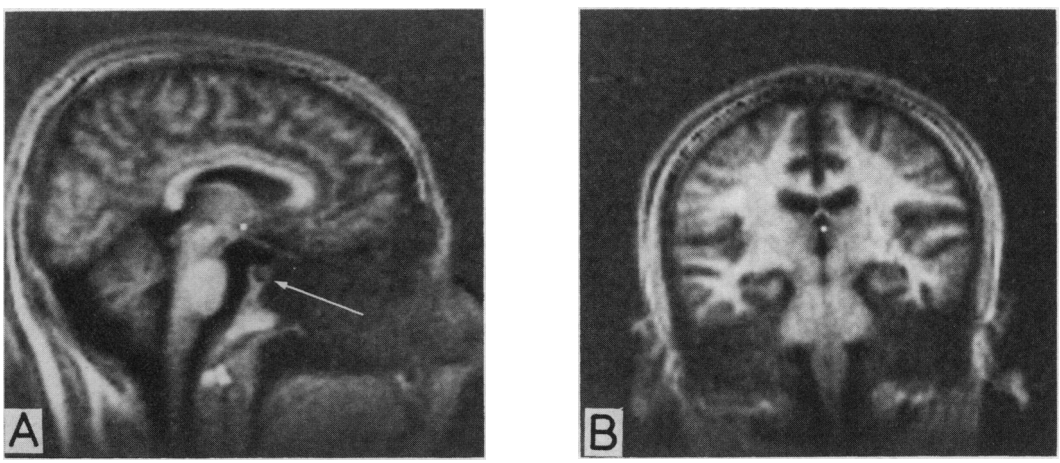

Figure 6. T_1 sagittal (A) and coronal (B) scans of the normal head. Detailed anatomical structure can be seen. The pituitary gland is arrowed

Heart

Movement of the heart produces unique problems in medical imaging: X-ray CT images are often difficult to interpret because of movement artefacts. Real-time ultrasound does allow visualization of the moving heart, and myocardial infarction can be inferred from dyskinesia, but pulmonary pathology may make visualization difficult. By contrast, NMR images of the heart are not degraded by overlying lung tissue or by movement artefact, although there is some blurring of edges (Hawkes *et al.* 1981*a*). However, if the data collection is synchronized with the pulse a sharper image is obtained (Figure 8). Blood has a long T_1 and so appears dark in the image, whereas the heart muscle has a relatively short T_1 and appears lighter, as do the papillary muscles.

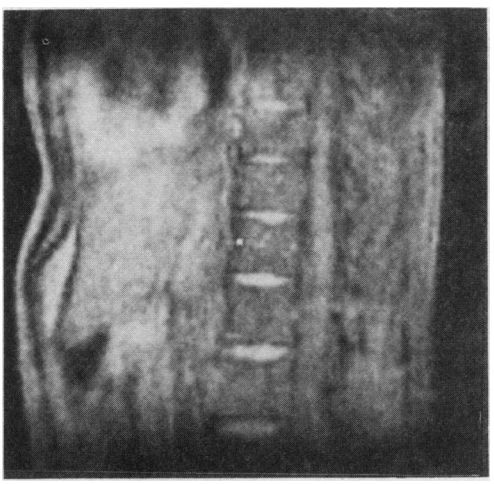

Figure 7. Sagittal section of the normal thoracolumbar spine. The vertebral bodies and intervertebral discs are seen. In addition, the nucleus pulposus and anulus fibrosus are distinguishable

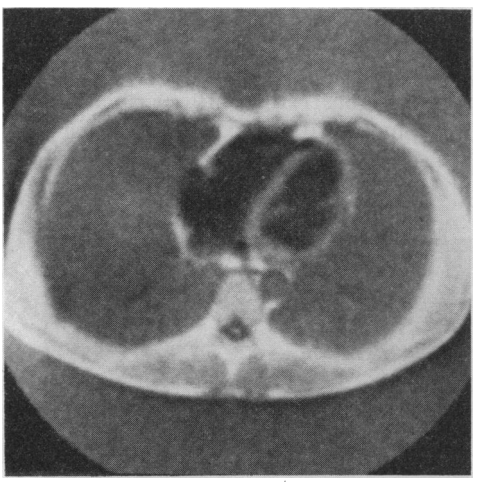

Figure 8. T_1 scan of the thorax of a normal subject. The data collection was synchronized with the pulse. The relatively thick-walled left ventricle and papillary muscles are seen. Posteriorly the spinal cord is seen surrounded by CSF which appears black

It has been found *in vitro* that ischaemic heart muscle has a prolonged T_1 (Williams *et al.* 1979), and initial studies *in vivo* suggest that myocardial infarction and ischaemia will be visualized by NMR. Diagnosis of congenital heart disease may also be possible (Heneghan *et al.* 1982).

Oxygen in solution is paramagnetic, and shortens the value of T_1. Thus oxygen may be used as a contrast agent (Young *et al.* 1982). If a patient breathes 100% oxygen, the T_1 of the left ventricular cavity is seen to fall. Further work on contrast agents in NMR continues.

Abdomen

T_1-dependent abdominal images allow the liver, spleen, kidneys, pancreas and major blood vessels to be seen. Respiratory movement causes only slight blurring of the anterior abdominal wall (Figure 9), and the artefact often seen on X-ray CT due to the gastric air bubble is absent.

The internal vascular structures in the liver can be seen, as can the gallbladder. Most hepatic pathology causes a prolongation of T_1 (Smith *et al* 1981*c*, Doyle *et al.* 1981*b*), although Wilson's disease, haemochromatosis and haemosiderosis tend to have shorter T_1 values, presumably related to deposited paramagnetic metal ions. Primary biliary cirrhosis, in which liver copper values are elevated, may also have a short T_1, with a characteristic NMR appearance (Doyle *et al.* 1981*b*).

The pancreas has a relatively short T_1 and so is often difficult to distinguish from adjacent

tissues. However, carcinoma of the head of the pancreas, pancreatitis, pancreatic pseudocysts and pancreatic abscess have been identified (Young *et al.* 1982, Smith *et al.* 1982).

The renal cortex and medulla are often distinguished in T_1-dependent scans (Figure 9), but in some cases of chronic glomerulonephritis this contrast is absent (Young *et al.* 1982). Focal renal disease such as cysts or carcinoma may also be seen with NMR (Smith *et al.* 1981*a*). Further work on renal disease is in progress.

Other areas

Using high-resolution NMR scans, retroperitoneal structures including the adrenal glands and lymph nodes can be identified (Young *et al.* 1982). Images of limbs may be obtained and these show the muscle groups and blood vessels. Exercised muscles show a prolongation of T_1 which may be related to increased blood flow.

Blood flow

The various NMR sequences involve data collection at some time after the application of the RF pulse. As flowing blood enters an NMR 'slice' without itself having been subject to the RF pulse applied to the slice, so the NMR characteristics of the blood will be distinct from those of surrounding tissues. This feature can be used to enhance blood vessels in scans with rapid data collection (Figure 10).

NMR can be used to measure blood flow (Singer 1981) and this may in future be available clinically.

Other uses

The initial experimental work on the medical use of NMR involved *in vivo* spectroscopy (Gadian & Radda 1981), which has enabled metabolic processes to be followed noninvasively. It may be possible to combine spectroscopy and imaging by NMR. NMR spectroscopy has been used to study other nuclei than protons, especially ^{31}P and ^{13}C. NMR imaging is possible with these nuclei, although they are much less abundant than hydrogen in biological systems and require a more powerful magnetic field. Images *in vitro* using ^{23}Na have also been obtained (Delayre *et al.* 1981) but, for the present, all medical NMR imaging uses hydrogen nuclei.

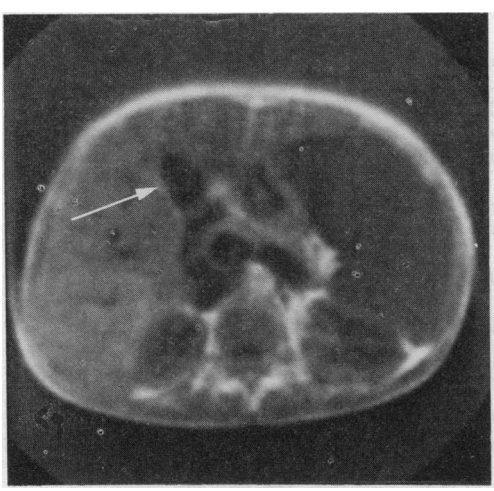

Figure 9. T_1 scan of the upper abdomen of a patient with hepatosplenomegaly due to leishmaniasis. The gallbladder is arrowed. Posteriorly the kidneys are visible, and the cortex and medulla are distinguishable

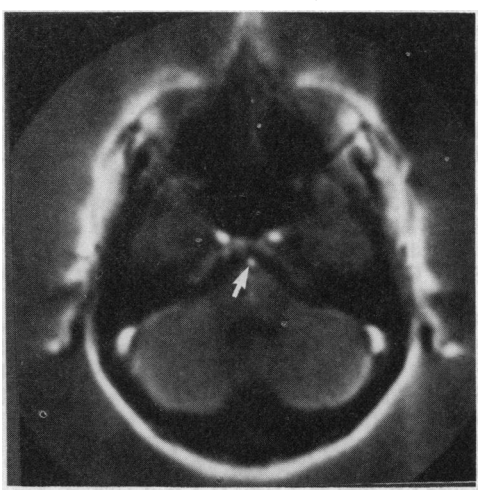

Figure 10. A proton-density scan of a normal subject at the level of the pons. This particular sequence enhances flowing blood. The basilar artery is arrowed, and anterior to it the carotid arteries are visible. More posteriorly and laterally the sigmoid sinuses can be seen

Conclusion

NMR imaging can give clinical information which, especially in neurology, promises to be of practical use. This information is not only anatomical, but also reflects physiological status and blood flow. In addition, the technique involves no exposure to ionizing radiation and seems to be harmless. There is little doubt that NMR imaging will soon have an established place alongside other major imaging techniques.

Acknowledgments: My thanks are due to the Department of Health and Social Security, particularly to Mr Gordon Higson and Mr John Williams for their support; and to Dr I R Young and his colleagues from Picker International for technical assistance. I would also like to thank Professor R E Steiner for his help.

References

Alfidi R J, Haaga J R, Elyousef S J *et al.* (1982) *Radiology* **143,** 175–181
Bailes D R, Young I R, Thomas D J, Straughan K, Bydder G M & Steiner R E (1982) *Clinical Radiology* **33,** 395–414
Bloch F (1946) *Physical Review* **70,** 460–474
Buonanno F S, Pykett I L, Kistler J P *et al.* (1982) *Radiology* **143,** 187–193
Bydder G M & Steiner R E (1982) *Neuroradiology* **23,** 231–240
Crooks L, Arakawa M, Hoenninger J *et al.* (1982) *Radiology* **143,** 169–174
Damadian R (1971) *Science* **171,** 1151–1153
Damadian R, Goldsmith M & Minkoff L (1977) *Physiological Chemistry and Physics* **9,** 97–100, 108
Delayre J L, Ingwell J S, Malloy C & Fossell E T (1981) *Science* **212,** 935–936
Doyle F H, Gore J C, Pennock J M *et al.* (1981*a*) *Lancet* ii, 53–57
Doyle F H, Pennock J M, Banks L M *et al.* (1981*b*) *American Journal of Roentgenology* **138,** 193–200
Edelstein W A, Hutchison J M S, Johnson G & Redpath T (1980) *Physics in Medicine and Biology* **25,** 751–756
Gadian D G & Radda G K (1981) *Annual Review of Biochemistry* **50,** 69–83
Hawkes R C, Holland G N, Moore W S, Roebuck E J & Worthington B S (1981*a*) *Journal of Computer Assisted Tomography* **5,** 605–612
Hawkes R C, Holland G N, Moore W S, Roebuck E J & Worthington B S (1981*b*) *Journal of Computer Assisted Tomography* **5,** 613–618
Heneghan M A, Biancaniello T M, Heidelberger E, Peterson S B, Marsh M J & Lauterbur P C (1982) *Radiology* **143,** 183–186
Hinshaw W S, Bottomley P A & Holland G N (1977) *Nature* **270,** 722–723
Holland G N, Hawkes R C & Moore W S (1980*a*) *Journal of Computer Assisted Tomography* **4,** 429–433
Holland G N, Moore W S & Hawkes R C (1980*b*) *Journal of Computer Assisted Tomography* **4,** 1–3
Hounsfield G N (1980) *Journal of Computer Assisted Tomography* **4,** 665–674
Lauterbur P C (1973) *Nature* **242,** 190–191
Mansfield P, Grannell P K & Maudsley A A (1974) Proceedings 18th Ampère Congress, Nottingham; pp 431–432
Mansfield P, Pykett I L & Morris P G (1978) *British Journal of Radiology* **51,** 921–922
National Radiological Protection Board (1981) *Radiography* **47,** 258–260
Purcell E M, Torrey H C & Pound R V (1946) *Physical Review* **69,** 37–38
Pykett I L, Newhouse J H, Buonanno F S, Brady T J, Goldman M R, Kistler J P & Pohost G M (1982) *Radiology* **143,** 157–168
Ross R J, Thompson J S, Kim K & Bailey R A (1982) *Radiology* **143,** 195–205
Singer J R (1981) In: Nuclear Magnetic Resonance Imaging in Medicine. Ed. L Kaufman *et al.* Igaku-Shoin Medical Publishers, New York; pp 128–144
Smith F W, Hutchison J M S, Mallard J R, Reid A, Johnson G, Redpath R W & Selbie R D (1981*a*) *Diagnostic Imaging* **50,** 61–65
Smith F W, Mallard J R, Hutchison J M S, Reid A, Johnson G, Redpath T W & Selbie R D (1981*b*) *Lancet* i, 78–79
Smith F W, Mallard J R, Reid A & Hutchison J M S (1981*c*) *Lancet* i, 963–966
Smith F W, Reid A, Hutchison J M S & Mallard J R (1982) *Radiology* **142,** 677–680
Steiner R E (1982) *British Medical Journal* **284,** 1590–1592
Weisman I D, Bennett L H, Maxwell L R & Woods M W (1972) *Science* **178,** 1288–1290
Williams E S, Kaplan J I, Thatcher F, Zimmerman G & Knoebel S B (1979) *Journal of Nuclear Medicine* **21,** 449–453
Young I R, Bailes D R, Burl M *et al.* (1982) *Journal of Computer Assisted Tomography* **6,** 1–8
Young I R, Burl M, Clarke G J *et al.* (1981*a*). *American Journal of Roentgenology* **137,** 895–901
Young I R, Hall A S, Pallis C A, Legg N J, Bydder G M & Steiner R E (1981*b*) *Lancet* ii, 1063–1066